Journal of Applied Polymer Science

Novel phase inversion process for symmetric membrane formation through thermal quenching of polymer solution in same solvent

Hsu-Hsien Chang,[1] Konstantinos G. Beltsios,[2] Hsuan-Fu Yu,[1,3] Yu-Hsuan Wu,[1] Liao-Ping Cheng[1,3]

[1]Department of Chemical and Materials Engineering, Tamkang University, New Taipei city, Taiwan, Republic of China

[2]Department of Materials Science and Engineering, University of Ioannina, Ioannina, Greece

[3]Energy and Opto-Electronic Materials Research Center, Tamkang University, New Taipei city, Taiwan, Republic of China

Correspondence to: L.-P. Cheng (E-mail: lpcheng@mail.tku.edu.tw)

ABSTRACT: A new and useful form of phase inversion for the formation of porous polymeric membranes is presented herein. As in the case of thermally induced phase separation (TIPS), this new form involves only two components (polymer and solvent) and a thermal quench; here the quench is accomplished via immersion in a cold bath of the micromolecular component (solvent) of the dope. In terms of a fixed-pressure two-component phase diagram the quench is a non-vertical one. We will refer to the new method as cold-solvent induced phase separation (CIPS). In the present work we study mainly the poly(ethylene-co-vinyl alcohol)/1,3-propanediol system which leads to bi-continuous structures stemming from a combination of liquid-liquid demixing and crystallization. In addition, we compare with the case of the Nylon-l2/formic acid system that we have briefly considered before and study further herein; the consequences of the TIPS to CIPS shift of method are different for the two systems, and the two situations are representative of two general possibilities. We also report general properties such as porosity, tensile strength, water permeation flux, and crystallinity of the produced poly(ethylene-co-vinyl alcohol) membranes. © 2015 Wiley Periodicals, Inc. J. Appl. Polym. Sci. **2015**, *132*, 42282.

KEYWORDS: crystallization; membranes; morphology; polyamides; porous materials

Received 27 December 2014; accepted 30 March 2015

DOI: 10.1002/app.42282

INTRODUCTION

Phase inversion is, as a result of combined simplicity and effectiveness, the most popular method for the preparation of porous polymer membranes.[1] There are several varieties of phase inversion, with the two most common ones being: (a) polymer/solvent/non-solvent phase inversion, coming in two main sub-varieties (wet phase inversion; WPI, and dry phase inversion; DPI), (b) thermally induced phase inversion (TIPS) which is based on a two component system (polymer/solvent) and a temperature shift under fixed pressure and overall-composition conditions.[2–11] Employment of additional components, the use of pressure changes, and various special processing steps are among the further options considered within the field of phase inversion.[3–11] In all cases, phase inversion amounts to the bringing of a single-phase concentrated polymer solution (known as the dope) into a proper multiphase (usually two-phase) regime, with the ensuing phase separation leading, upon simple further processing, to a porous polymeric membrane.

The WPI version is the most versatile of the aforementioned varieties. WPI is capable of yielding from nearly symmetric to highly asymmetric membranes. The eventual destiny of the used bath (containing non-solvent and accumulated solvent) is an issue of concern; the two components might be processed for recovery or the bath might be disposed, for example following neutralization, as in the case of strong acid/water binary bath. The DPI requires the employment of a solvent with volatility substantially higher than that of the non-solvent, while viscosity-enhancing additives are frequently necessary. In addition to the membrane, two fluid phases that require further processing need to be collected. The TIPS version is applied mostly to crystallizable polymers, some elaborate processing equipment is often necessary and the outcome is a symmetric membrane; mildly asymmetric versions are possible through extended approaches requiring special processing.[12–22]

In this work we present a new and useful variety of phase inversion. The employment of a two component system and a thermal quench are features shared with TIPS, while the employment of a bath that can alter dope composition is the feature shared with WPI. However, it worth noting that the liquid of the bath is not a conventional non-solvent, as in WPI, but the same solvent as that found in the dope. Hence, the new method (termed cold-solvent induced phase separation; CIPS) can be thought as thermal quench that can be modified by a

compositional drift; hence, the path for the quench, in terms of a fixed-pressure two-component phase diagram, a non-vertical one. The possibility to prepare porous membranes having structures different from those obtainable either by TIPS or via coagulation in usual non-solvent baths is intriguing as regards the range of available processing and structure-controlling processing parameters. In addition, the practical significance of this new and potentially widely applicable membrane fabrication option should not escape attention. The employed membrane forming system consists only of a polymer and its solvent, and hence the precipitation bath can be used repeatedly, as opposed to the nonsolvent-solvent-polymer membrane forming systems, for which the maintenance of a stable bath composition is always a difficult yet crucial task for reproducible structural outcomes. Finally in case the membrane structure does not change substantially upon shifting from TIPS to CIPS, it is technically simpler to quench the dope in a reusable bath rather than through a heat exchange processes that necessitates encasement of the dope in a special closed cell. Also it is easier to fabricate hollow fiber versions of the membranes etc. The lower bound for quench temperature is that of the melting point of the solvent while the, usually less important for CIPS, upper bound is some temperature below the boiling point of the solvent.

We explore in detail an application of the CIPS method to the poly(ethylene-co-vinyl alcohol) (EVOH)/1,3-propanediol system and compare with the outcome of the TIPS method. Morphology is studied via high resolution scanning electron microscopy and, in addition, tensile strength, crystallinity, and water permeation flux of the membranes were measured by appropriate techniques. The results suggest that the currently developed membranes have potential to serve in micro-filtration processes. For CIPS versus TIPS comparison purposes we also consider the morphological details of a second system (Nylon-12/formic acid; FA). We include a qualitative framework of potential thickness changes that might affect the outcome of CIPS processing and compare with the TIPS case.

METHODS

Material

EVOH polymer (EVOH 32, $M_n = 21{,}500$ g/mole, $\rho = 1.19$ g/cm^3) was purchased from Aldrich. 1,3-Propanediol (Aldrich, reagent grade) was used as a solvent for EVOH. Nylon-12 polymer (Grilamid Nylon-12, L20G, $M_n = 24{,}000$ g/mole, $\rho = 1.03$ g/cm^3) was purchased from Emser Werke Inc. and FA (Aldrich, reagent grade) was used as solvent. All materials were used as received.

Phase Diagram Determination for the 1,3-Propanediol/EVOH System

The gelation phase boundary for the binary system, 1,3-propanediol/EVOH was determined by the cloud point method, as reported previously.[23] Briefly, a specific amount of polymer (dried in an oven at 60°C) was mixed with the diluent (latent solvent) and sealed in a glass bottle with a Teflon-lined cap. The mixture was blended at an elevated high temperature until the polymer was completely dissolved. The formed solution was then put in a thermostat maintained at constant temperature. After standing for 14 days, the sample was inverted to see whether gelation has occurred. The gelation points in the phase diagram were identified as the compositions at which homogeneous solutions began to gel.

Table I. Physical Constants Used for Binodal and Spinodal Calculations

Physical Constants	1,3-Propandiol/EVOH System
V_1 (cm^3/mol)	72.4
V_2 (cm^3/mol)	18067
V_u (cm^3/mol)	65.5
r	250
ΔH (J/g)[a]	174
T_m (°C)[b]	184

Calculated interaction parameter $\chi = -0.622 + \frac{380.2}{T}$
EVOH, poly(ethylene-co-vinyl alcohol).
[a] Average value of literature data.[43, 44]
[b] Measured by DSC.

The liquid-liquid demixing boundaries (binodal and spinodal) were determined theoretically following the approach of McGuire *et al.*[20] The melting point of the binary diluent/polymer system can be expressed as:

$$\frac{1}{T_m} - \frac{1}{T_m{}^o} = \frac{RV_u}{\Delta H_u V_1}(\phi_1 - \chi\phi_1{}^2) \quad (1)$$

where T_m and $T_m{}^o$ are the melting temperatures of the crystalline polymer in solution and the solid states, respectively, V_1 is the molar volume of the solvent, V_u is the molar volume of the repeat unit, ΔH_u is the heat of fusion for the repeat unit, ϕ_1 is the volume fraction of the solvent, and χ is the Flory–Huggins interaction parameter for the polymer-solvent binary pair. Equation (1) was used to calculate the interaction parameters between 1,3-propanediol and EVOH at different temperatures, using the measured crystallization compositions. The obtained χ values were then substituted into the binodal [eq.(2)] and spinodal equations [eq.(3)] given below to solve for these two phase separation boundaries in the phase diagram.[19, 20]

$$\left[(\phi_2{}^\beta)^2 - (\phi_2{}^\alpha)^2\right]\chi = ln\frac{1-\phi_2{}^\alpha}{1-\phi_2{}^\beta} + (1-\frac{1}{r})(\phi_2{}^\alpha - \phi_2{}^\beta)$$

$$r\left[(1-\phi_2{}^\beta)^2 - (1-\phi_2{}^\alpha)^2\right]\chi = ln\frac{\phi_2{}^\alpha}{\phi_2{}^\beta} + (r-1)(\phi_2{}^\alpha - \phi_2{}^\beta) \quad (2)$$

where $\phi_2{}^\alpha$ and $\phi_2{}^\beta$ are the volume fractions of polymer in separated phases α and β, respectively. r is the molar volume ratio of the polymer to the solvent.

$$\frac{1}{(1-\phi_2)} + \frac{1}{r} - 1 - 2\chi\phi_2 = 0 \quad (3)$$

where ϕ_2 is the composition of polymer in the spinodal. The physical constants used for calculations are listed in Table I.

Membrane Preparation and Characterization

Membrane Preparation by the CIPS Method. EVOH membranes were prepared in the form of a flat sheet by the CIPS method. EVOH was dissolved in 1,3-propanediol at 130°C on a roller to form a 20 wt % homogeneous solution. The solution was put in a constant temperature oven (80°C) for the period

of 0.5 h and then cast on a glass plate using a casting knife with a clearance of 400 μm. Following casting, the solution was immersed in the same solvent as that for preparing the dope at a low temperature to induce polymer precipitation. The formed nascent EVOH membrane was washed in water, and then freeze-dried.

Membrane Preparation by the TIPS Method. EVOH membranes were also prepared by the TIPS method for comparison with CIPS. The polymer was dissolved in 1,3-propandiol to form a 20 wt % homogeneous solution at an elevated temperature. The solution was cooled to room temperature and then an appropriate amount of the formed gel was placed in a cell for the subsequent quenching step. The cell consists of two stainless steel plates and a Teflon sheet having a square opening in the center (cf. Ref. 23 for the cell design). The Teflon sheet was sandwiched between the stainless steel plates to give a space of constant height. The sample was heated at a high temperature in an oven for 30 min to ensure complete dissolution of the polymer gel. Then, it was immersed in an isothermal water bath at 23 ± 2^{o}C to induce phase separation. The nascent membrane was washed and then dried by the same procedure as that used in the CIPS method. The Nylon-12/ FA TIPS and CIPS membranes were prepared similarly to the corresponding EVOH/1,3-propandiol membranes, starting with the formation of a 20 wt % homogeneous solution at 80°C; for more details see reference.[24]

Membrane Characterization. The formed membranes were characterized by the following methods.

a. Morphologies of the membranes were observed using a field emission scanning electron microscope (FESEM, Leo 1530, Carl Zeiss, Oberkochen, Germany). Membrane samples were vacuum-dried and then an appropriate size of the top surface, bottom surface, or cross sectional area was attached to a sample holder using conductive cooper tapes. The cross section was obtained by fracturing the membrane in liquid nitrogen. Silver paste was applied at the edges of the sample to enhance electronic conductivity. Then, the sample was sputtered with a layer of Pt-Pd alloy (~2 nm) and observed under a low acceleration voltage (2.5 kV) by means of an in-lens detector. The cross section of the membrane was obtained by fracturing the membrane in liquid nitrogen. It was then vacuum-dried and attached to a sample holder by conductive copper tapes. Silver paste was applied at the edges of the sample to enhance electronic conductivity. For the top and bottom surfaces, a piece of membrane was vacuum-dried and then attached to a sample holder by conductive copper tapes. Then, the sample was sputtered with a thin layer (~2 nm) of Pt-Pd alloy and observed under a low acceleration voltage, 2 kV, by means of an in-lens detector. The pore and particle sizes in the SEM photographs were measured based on the calibrated scale.
b. The porosity of the membrane was determined by the following equation:

$$\text{Porosity } (\%) = \left[\left(V_m - V_p\right)/V_m\right] \times 100\%$$

where V_m is the bulk volume of the membrane and V_p is the volume of polymer in the membrane. V_m was obtained by multiplying the membrane area by its thickness, as was measured by a thickness gauge. V_p is equal to W_m / ρ_p, where W_m is the weight of the membrane and ρ_p is the density of the polymer ($\rho_p = 1.2$ g/cm^3 for EVOH-32 and $\rho_p = 1.03$ g/cm^3 for Nylon-12).
c. The tensile strength at the breaking point for various membranes was determined using a universal testing machine (AGS-J SHIMADZU, Kyoto, Japan) following ISO 37 type III. At least 5 samples were examined for each membrane, and the average value was reported with deviation.
d. Pure water fluxes of the prepared membranes were measured using a dead-end type filtration system (effective area 11.34 cm^2) over the trans-membrane pressure range of 100–400 kPa, corresponding to micro- and ultra-filtration operations. The membrane was pre-wetted in 2-propanol first, and then its water fluxes were measured at room temperature. For each measurement, water was collected after stable flux being attained; the collection time was ca. 1–30 min, depending upon the efflux rate.
e. The structure of EVOH crystals in the membrane was determined by a wide angle X-ray diffractometer (XRD, D8 Advance, Bruker, Karlsruhe, Germany). The operational parameters consisted of source intensity = 40 kV/40mA, λ = 1.54 Å (copper K_α line), source slit width = 0.6 mm, increment = 0.05°/step, scanning speed = 3 s/step, and scanning range = $10^o < 2\theta < 30^o$. Crystallinity of the sample was determined by deconvolution of the diffraction peaks into amorphous and crystalline contributions, following a curving fitting method described in the literature.[8,25] The curve fitting scheme incorporated Gaussian and Lorenztian functions in a mixed mode by means of a commercial software, GRAMS/AI^{TM}.
f. The nominal pore sizes of the membranes were measured by the bubble-point method.[1,26] The membrane sample was cut into circular shape (3.8 cm in diameter) and wetted by the IPA solution first. This solution was a standard wetting medium, for which surface tension was adjusted to 21.7×10^{-3} N/m. Then the fully wetted sample was placed in the sealed sample chamber. Nitrogen gas was then allowed to flow into the chamber behind the sample. When the pressure reached a point that could overcome the capillary force of the fluid within the largest pore, the bubble point was obtained.

RESULTS AND DISCUSSION

Phase Diagram of the EVOH/1,3-Propanediol System

The phase diagram for the binary EVOH/1,3-propanediol system is shown in Figure 1. The filled squares (■) stand for the gelation points determined by the cloud point experiments. Connection of these points forms the phase equilibrium boundary of the binary system. Above the gelation line is a single phase zone, in which homogeneous polymer solutions can be prepared with long-term stability. On the other hand, a dope with composition below the gelation line will precipitate via solid-liquid demixing (i.e., crystallization) and/or liquid-liquid demixing (crossing the binodal or spinodal) into a gel. However, since liquid-liquid phase separation was not observed for all studied samples in the cloud point experiments, the binodal

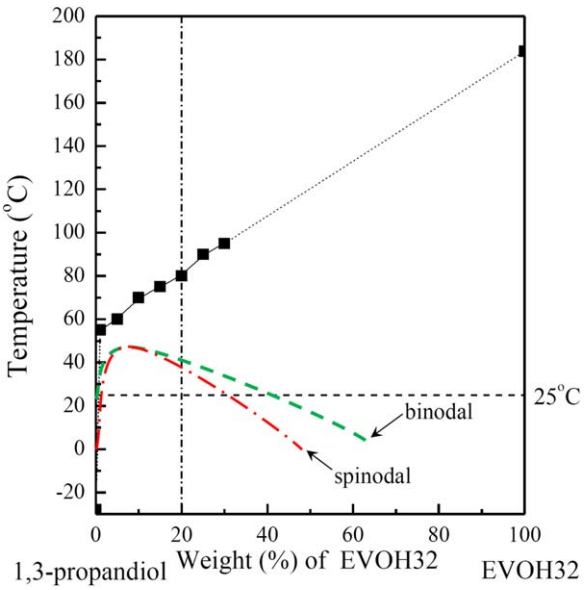

Figure 1. Phase diagrams for the 1,3-propanediol/ poly(ethylene-co-vinyl alcohol) (EVOH) system. ■, measured gelation points. Binodal and spinodal were determined based on Flory–Huggins theory. [Color figure can be viewed in the online issue, which is available at wileyonlinelibrary.com.]

and spinodal for this system are expected to locate below the gelation line, which is consistent with the calculated results shown in Figure 1.

CIPS and Processes Affecting Dope Thickness

Here we discuss the various processes that can affect dope/membrane thickness during membrane fabrication that involves CIPS; some comparisons with TIPS are included. From the "change of dope volume" point of view we can distinguish three general "stages" [stages (a), (b) and (c)] pertinent to CIPS-based membrane fabrication. Processes are assigned to stages on the basis of time they might start to operate (some processes might continue to operate during a subsequent stage); the processes can overlap and interact but we limit our discussion to the presentation of a "qualitative first map".

The suggested three stages and corresponding processes are as follows:

a. Stage of primary non-vertical quench effects; here dope volume changes while dope temperature still changes. We distinguish further:
   a1. Soret effect processes (see below).
   a2. Dope volume (thickness) change consequences of early phase separation stages in the case of *fast* phase separation processes, such as spinodal decomposition (SD). Further, regardless of whether fast phase separation processes operate, the chains in semi-concentrated solution states might preserve at high temperatures with small scales non-Gaussian ("swollen chain") exponents[27] while, upon quenching, they will start shrinking as soon as temperature starts to drop ($\chi\uparrow$). The latter microscopic shrinking of chain dimensions might either lead to some squeezing out of the solvent from the dope [a potential (a3) process; see below] or, at least, create conditions favorable for solvent squeezing out at a next (phase separation) stage [stage (b); see below].
   a3. Process (a3) is a dope response to temperature lowering; it can proceed (via mass transport) during cooling but it does not *necessitate* (as for example Soret effect does) the presence of intra-dope temperature gradients, since it is conceivable even in the theoretical case of temperature lowering in a spatially *uniform* fashion.
   a4. A process that might start to operate well before phase separation (especially if phase separation is a slow process) and can be described, at least approximately, in quasi-osmotic terms: the top of the dope acts approximately as equivalent to a semipermeable membrane (even while the chains form a *transient* mesh); only the solvent component can be exchanged and the usual result should be a net solvent flux *towards* the dope (hence, this is a process that usually favors dope expansion).
b. Stage of dope volume changes when temperature has become practically uniform while phase separation and other restructuring processes progress; the latter processes include intermediate and late stages of fast phase separation and, possibly, the bulk of slower phase separation and other restructuring processes (e.g. partial crystallization of polymer-rich domains in the case of interest). Stresses developing during phase separation and other restructuring leading to the gradual formation a solid network will normally favor the expulsion of an amount of micromolecular component in the dope to the bath; i.e. process (b) favors dope shrinkage. It might be noted that in an obliquely related phase inversion situation it was shown experimentally[28] that phase separation and/or chain shrinking favors dope contraction and expulsion of solvent, which because of certain spatial restrictions might lead to the formation of macrovoids (i.e. the solvent can be expelled either outside the dope or more locally, within the dope contour, in which case it can form macrovoids).
c. Stage that follows completion of phase separation and remaining isothermal restructuring processes. Here volume changes are possible as a result of subsequent processing, such as drying of CIPS products, for the generation of a liquid-free porous membrane. For a given membrane material, a given drying liquid, and comparable porous network geometries, the capillary force that favors compaction would be inversely proportional to the pore radius while the stronger such forces (i.e. the smaller the pores) are the more possible the reduction of porosity might be. Pinnau and Koros[29] have discussed the idea especially for the compaction of skin in certain phase inversion membranes, while some references therein are also good sources for related subjects.

In general it is nearly impossible to estimate safely the magnitudes of dope volume changes for most of the (a)–(c) stages theoretically while specially designed experiments will be necessary for corresponding experimental evaluations. What can be evaluated more easily is the combined outcome of the (a)–(c)

processes; the latter sum can be estimated upon determination of porosity and evaluation (e.g. from degree of crystallinity data) of the solid density of the final product and this is also, more or less, so in the case of related WPI questions, despite some attempts and half a century of pertinent experimental observations. In the case of present interest (CIPS) even the sign (net flow direction) of one of the contributions (Soret effect; see below) cannot always be predicted on safe theoretical grounds.

Let us now consider the Soret effect (a1); for a binary system this is the occurrence of a net mass flux of a component caused upon application of a temperature gradient to an, initially compositionally homogeneous, binary system. Detailed discussions are usually case specific; examples include the Semenov and Schimpf model[30] for certain classes of liquid systems and the careful discussion that Shewmon[31] offers for metal crystalline "matrices".

Semenov and Schimpf consider dissolved isolated polymer chains or suspended particles in a micromolecular fluid and emphasize the role of macroscopically oriented pressure gradients in the micromolecular fluid "matrix" as a result of the temperature dependence of various properties of the solvent. However, for polymer solutions containing mutually entangled polymer chains (as those of direct present interest) it appears more appropriate to focus on the small solvent molecules moving within a transient mesh of chains; cooling of one part of the solution will lower the quality of solvent and hence shrinkage (with enhancement of local polymer chain concentration) of the corresponding part of the mesh is expected.

A comparison of the TIPS and CIPS cases is of interest. In the case of TIPS with similar cooling from the two broad faces of the dope one might predict a tendency for the development of more concentrated zones near the cold surfaces of the solid cell and a less concentrated zone towards the mid-plane of the dope. When temperature equilibrates, the compositional gradients and their potential membrane structure consequences will be gradually eliminated, unless phase separation takes place fast enough (before elimination of compositional inhomogeneity along dope thickness); in the latter case some mild variation of morphology along the thickness might be detectable.

The case of CIPS can be different, especially if initially there is *one* dope side that is substantially colder than the other; the colder side will be the one in direct contact with the cold solvent bath (the early differentiation of temperature for the two broad sides will be smaller for thinner and more heat conductive supports of the dope). Let us now consider the case that the dope side adjacent to the bath is, initially, substantially colder. The solvent molecules of the latter (colder) side of the dope can move towards the bulk and warmer part of the dope, while a different, lower viscosity (hence, possibly, preferable), path option also exists: the colder part of the dope can shrink and expel some solvent to the solvent bath side. In the latter case a dope thickness reduction is possible (and morphological imprint of it might be preserved in the membrane in case of timely phase separation etc); the particular shrinkage process has no TIPS counterpart. Further, as the cold bath side of the dope is 'free' (in contact with a fluid) in CIPs while it is attached to the inside cell wall in TIPS, the (b) shrinkage process is also easier for CIPS. Processes of the (c) type are possible for both TIPS and CIPS though the contribution need not be the same (for the same dope composition and same starting and final temperatures) *if* different microstructures (e.g. because of dope composition changes upon shrinkage during phase separation) have developed before (c).

Finally, certain early gelation processes (e.g. through limited polymer crystallization) during quenches might lead to modifications of the picture described so far; e.g. in the case of an encased dope (as in TIPS) solvent can be released between case walls and the gelled dope under conditions that this is unfavorable for a liquid dope.

Overall, both similar and dissimilar microstructures and/or porosities appear possible for corresponding CIPS and TIPS cases. One might expect that the porosity for CIPS compared to that for TIPS will often be similar or lower since in some cases additional dope shrinkage mechanisms exist in the case of CIPS; however when the key reason for shrinkage is (c), which is strongly affected by morphology, we cannot exclude the occasional possibility of a CIPS structure that will be more prone to shrinkage than the corresponding TIPS structure.

In subsequent sections we will refer to few details of the preceding framework which as a whole should guide the design of future probing experiments. Also we might note that because of the emphasis on dope volume changes, the discussion does not pay enough attention to some important CIPS issues; hence structure formation processes are considered subsequently on a case-specific basis (Morphologies of the CIPS and TIPS membranes Section). In addition, there can be a substantial free convection effect for horizontal or near horizontal dopes[32]; hot and cold microstreams can move, respectively, preferably upwards and downwards. Such processes might not affect directly the thickness of the dope but they accelerate transport processes and, for example, they will affect the time that (b) processes begin.

For the interpretation of CIPS and TIPS observations for the two systems considered herein, we will also employ (Formation of Porous membranes by the CIPS method Section) a more phenomenological and/or less detailed approach that focuses on the relative contributions of heat and mass transfer to membrane structure formation.

Morphologies of the CIPS and TIPS Membranes

EVOH membranes were prepared by the CIPS method. The dope solution at 80°C was immersed in a 1,3-propanediol bath maintained at 23 ± 2°C. Figure 2(a) shows a full cross sectional SEM image of the formed membrane. It is a reasonably uniform porous structure and hence it is possible that the bulk of the liquid–liquid phase separation events took place within a limited range of compositions and temperatures; yet it should be noted that there are some traces of porosity at different scales; the latter characteristic has been attributed to multistep liquid-

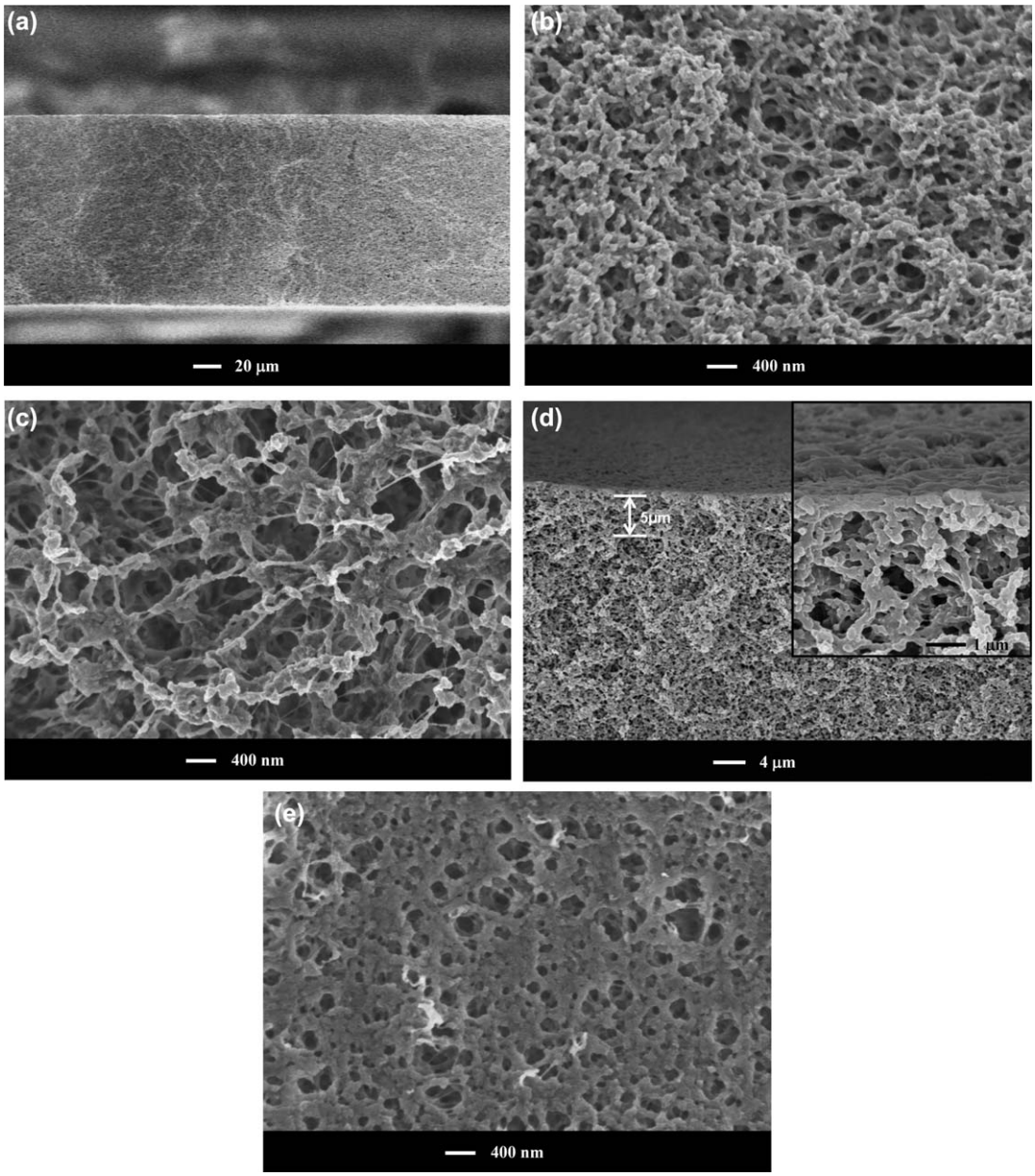

Figure 2. Morphology of the EVOH membrane formed by immersing a 20 wt % dope at 80°C in pure 1,3-propanediol at 25°C (cold-solvent induced phase separation; CIPS). (a) Total cross section; (b) high magnification of (a); (c) top surface; (d) region just underneath the top surface; and (e) bottom surface.

liquid phase separation in the case of WPI[33] and a related situation is conceivable here.

As regards the phase separation mode (or at least the dominant mode), high magnification near the central region, c.f., Figure 2(b), indicates a bi-continuous morphology, in which a porous network and a delicate solid polymeric network interweave to give a lacy-like appearance. Such type of structure is typically derived from SD occurring in a dope that has been quenched into the unstable region of the phase diagram, cf. Figure 1.[23,34,35] However, because the binodal and spinodal are submerged (located below the gelation line), partial polymer crystallization is also possible and indeed has occurred as evident from differential scanning calorimetry (DSC) and XRD measurements and the particulate entities found in the lacy skeleton [Figure 2(b)]. As regards the sequence of phase separation events, the morphology suggests that SD and subsequent coarsening has taken place earlier and dominated the precipitation process; i.e. SD initiates and propagates rapidly to set-in the framework of the polymeric matrix, while crystallization follows in the polymer-rich phase. This precipitation scheme is consistent with the fact that SD is a spontaneous process, while for crystallization there is an activation energy barrier to overcome. During SD separation and subsequent ripening of the SD-derived structure, crystallization may occur

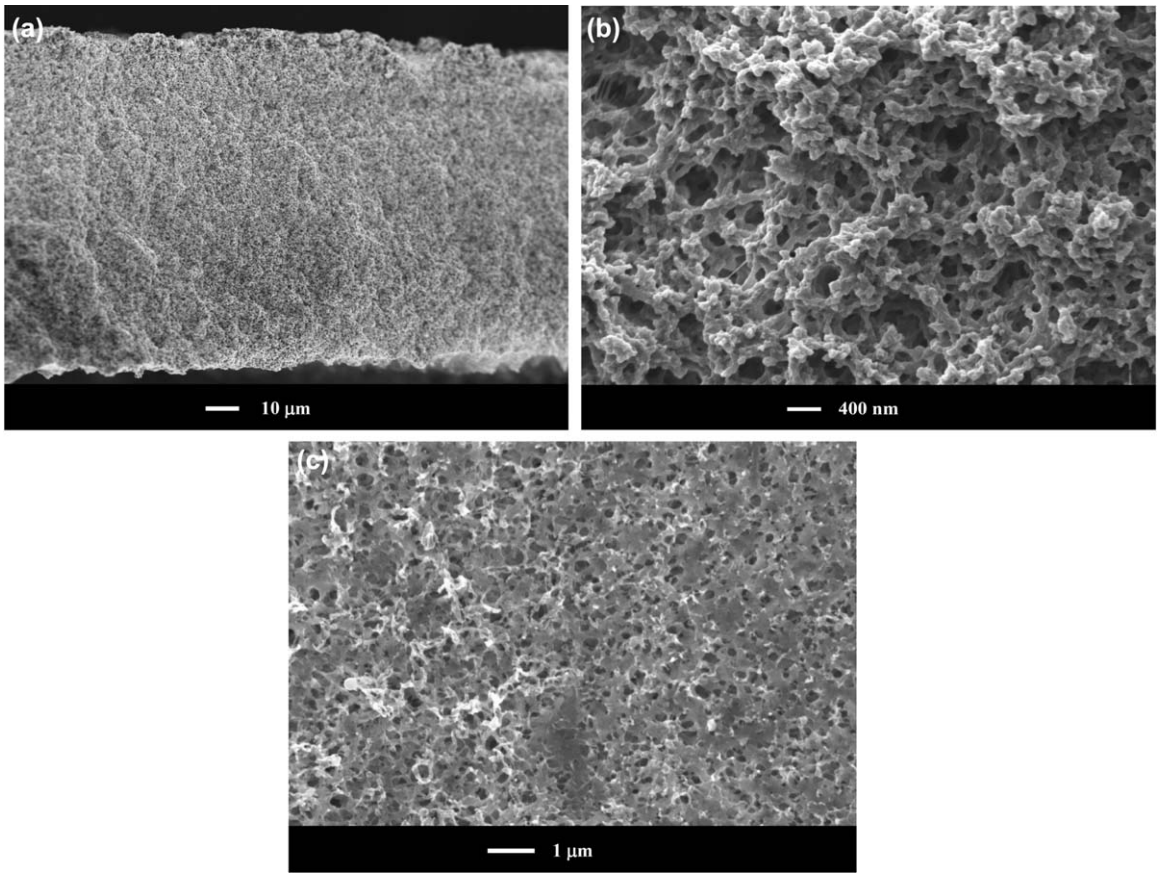

Figure 3. Morphologies of the EVOH membrane prepared by the thermally induced phase separation (TIPS) method. (a) Total cross section; (b) high magnification of (a); (c) surface. Polymer concentration in the dope was 20 wt % and temperature of the quench bath was 25°C.

and eventually fix the microporous structure. Furthermore, as shown previously,[23] if crystallization was deliberately promoted by introduction of nuclei during a dope-aging step or by quenching the dope at temperatures higher than the spinodal, the formed membrane should consist of globular semi-crystalline entities in a reasonably sturdy packing.

The top surface of the membrane, as shown in Figure 2(c), also exhibits the bi-continuous lacy morphology as in the cross sectional region. However, the pores here are somewhat larger, suggesting that polymer concentration in this region is lower at phase separation. However, close inspection of the cross-sectional structure near the top surface, Figure 2(d), indicates that the dilution zone is quite short (<2μm). Hence, with the exception of a narrow top zone it is possible that that at the time of the main events of structure formation, composition and temperature do not vary substantially with depth. A modified morphology is also found at the bottom [Figure 2(e)]; similar structural features are also observed in the case of WPI semi-crystalline membranes, and the pertinent densified/flattened morphology is resulted from the limitations imposed by the solid glass plate/substrate.[7,9,24]

Morphologies of the membrane prepared by TIPS with the same dope and quenching temperature have been demonstrated previously.[23] In Figure 3, typical cross sectional and surface images are illustrated for comparison; the CIPS and TIPS structures do appear comparable and they also exhibit comparable porosities (56.76 ± 1.8% for CIPS, 54.42 ± 2.7% for TIPS), degrees of crystallinity and water fluxes (see Formation of Porous membranes by the CIPS method Section for a presentation of the properties of EVOH membranes made via CIPS). Hence, it is possible that the CIPS [Figure 2(b)] and TIPS (Figure 3) structures are formed under comparable conditions. The similar level of shrinkage for

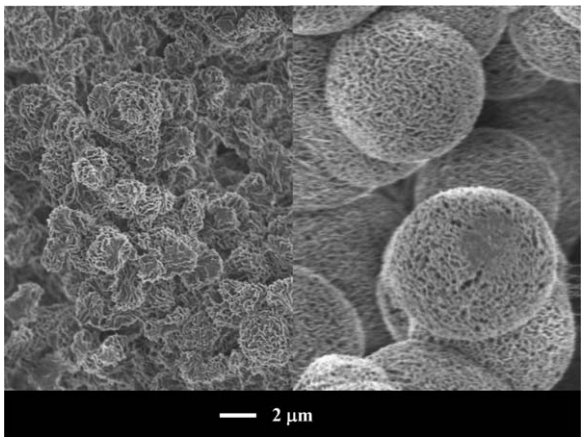

Figure 4. Cross sectional morphologies of the Nylon-12 membranes prepared by the CIPS (left) and TIPS (right) methods. Polymer concentration in the dope was 20 wt % and the quenching temperature was 10°C.

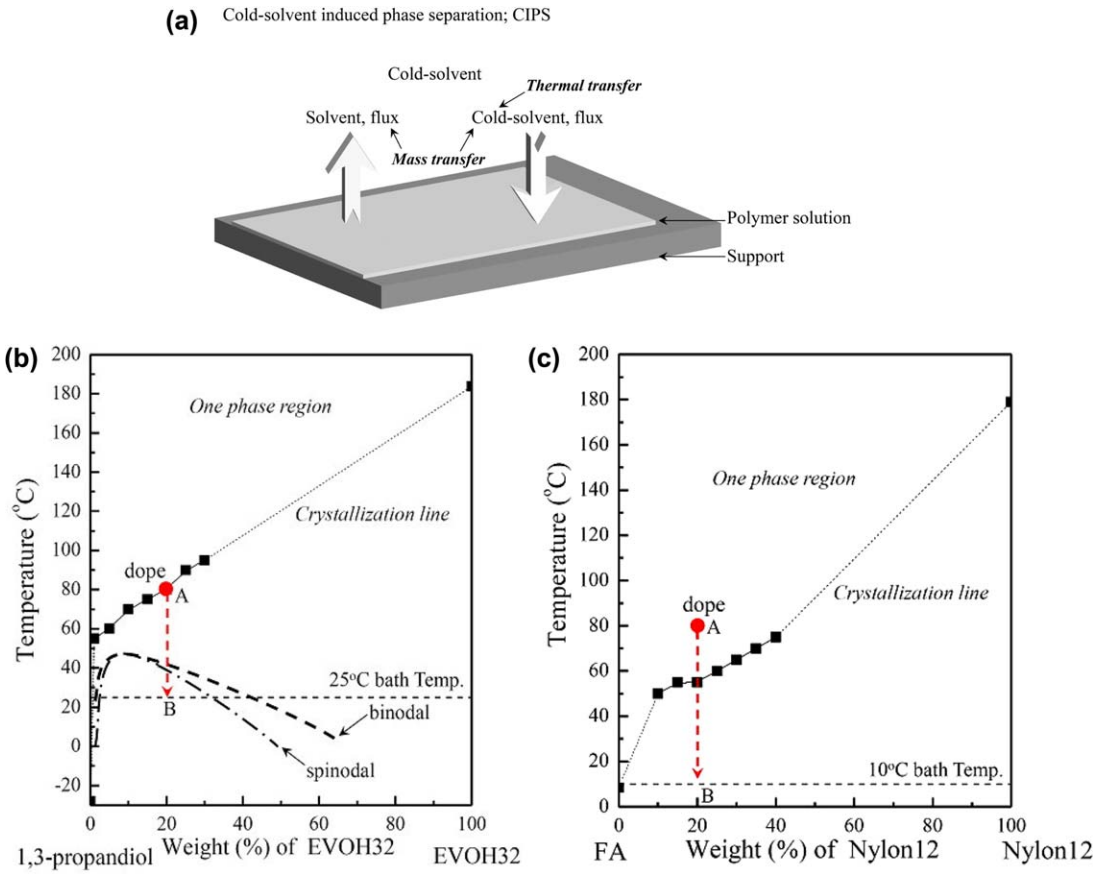

Figure 5. Mechanism of porous membrane formation by CIPS. (a) Scheme of mass and thermal transfer occurring at the film/bath interface; (b) the 1.3-propandiol/EVOH system which gives comparable CIPS and TIPS structures; (c) the formic acid/Nylon-12 system which gives different CIPS and TIPS structures. Actual quenches are not vertical and in the case of CIPS there can be deviations in either directions (high solvent and high polymer sides); see text for details. [Color figure can be viewed in the online issue, which is available at wileyonlinelibrary.com.]

CIPS and TIPS membranes despite the involvement of *fast* structure formation processes (such as SD phase separation) might be attributed to the quick dope gelation (even largely before entrance to the submerged binodal); see CIPS and processes affecting dope thickness Section for details.

In a previous publication[24] membrane preparation for the Nylon-12/FA system, with an emphasis on TIPS, was reported. Unlike the EVOH/1,3-propanediol system, the CIPS and TIPS gave rise to substantially different morphologies when applied to the Nylon-12/FA system. As shown in Figure 4, the CIPS-membrane consists of a packing of small globules with a typical diameter of ~1.5 μm, while the TIPS-membrane consists of a packing of larger globules of ~10 μm; in addition there is a difference as regards the porosity level which is 59.73 ± 0.98% for CIPS and 67.12 ± 2.40% for TIPS. The difference of the two systems as regards the similarity/dissimilarity of the CPIS–TIPS structures) will be considered on the basis of the phenomenological scheme based on the relative contributions of heat and mass transport to morphology development. Before that (Formation of Porous membranes by the CIPS method Section) we will consider the porosity difference of the CIPS and TIPS Nylon-12/FA membranes. In the case of the Nylon-12 membranes, we note that the structures are of comparable general type of geometry (packings of globules) and hence a simplified comparison can focus on scale. Compared to the TIPS structure the CIPS structure contains globules and main pores smaller by a factor of ca. 6 ± 1; hence capillary forces favoring shrinkage are higher by a factor of 6 ± 1 (see CIPS and processes affecting dope thickness Section) in the case of the CIPS structure. We lack the detailed data necessary for the assessment of the contribution of different extents of the (a) and (b) processes while we note that, at least sign-wise, the observed difference as regards porosity is compatible with the effect possible because of the (c) process effect.

Formation of Porous Membranes by the CIPS Method

Polymeric membranes formed by the CIPS method demonstrate morphologies stemming from crystallization and/or liquid-liquid phase separation (plus coarsening). Phase separation is induced by means of the cold solvent. When the high temperature polymer solution contacts the cold solvent, at the point of immersion both heat transport and mass transport (that can be diffusional and convective) take place [Figure 5(a)]. In our case what is of direct interest is the extent of the heat and mass transport processes accomplished up to and also during the period of membrane structure formation via liquid-liquid phase separation (plus coarsening) and crystallization. We will

Table II. Preparation Conditions[a] and Properties for EVOH and Nylon-12 Membranes

Polymer[a]	Method	Temperature (°C)	Porosity[b] (%)	Pore Radius[c] (μm)	Crystallinity[d] (%)
EVOH32	CIPS	23	56.76 ± 1.8	1.67 ± 0.36	38.8
	TIPS	23	54.42 ± 2.7	1.55 ± 0.47	39.4
Nylon-12	CIPS	10	59.73 ± 0.98	8.51 ± 0.98	38.4
	TIPS	10	67.12 ± 2.4	-	36.2

CIPS, cold-solvent induced phase separation; EVOH, poly(ethylene-co-vinyl alcohol); TIPS, thermally induced phase separation.
[a] Dope: 20 wt % EVOH32 in 1,3-propandiol at 130°C; 20 wt % Nylon-12 in FA at 80°C.
[b] Calculated based on the density of EVOH32 (1.2 g/cm^3) and Nylon-12 (1.03 g/cm^3) and the measured mass and thickness of the membrane.
[c] Bubble-point method, maximum pressure 392 kPa.
[d] Amorphous and crystalline regions being sorted by curve fitting technique.

consider two broad cases with our two experimental systems constituting potential corresponding examples.

As a general guide we note that mass diffusivity in a liquid system is, even for small molecules, smaller (e.g. by two orders of magnitude) than heat diffusivity and, hence, for comparable relative deviations from homogeneity over the same distance and with the system moving towards homogenization because of appropriate boundary conditions, the elimination of compositional inhomogeneity will happen much more slowly (e.g. during a time period longer by two orders of magnitude) than the elimination of temperature inhomogeneity. Hence, if structure formation processes occur quickly during the CIPS quench, the heat and mass transport contributions cannot be comparable, if intra-dope mass and heat transport occur by diffusional processes alone. Here, the compositional gradient point of view constitutes is an oversimplification. While at the completion of the CIPS process, there will be no temperature gradients, the mesoscopic scale concentration (mass/volume) of the solvent will be different inside and outside the dope and, in principle, it might even vary within the dope, in case that the porosity varies with the distance from the surface of the membrane. More accurately, during CIPS there will be gradients of the chemical potential of the solvent both before and after temperature equilibration, while at the completion of CIPS the chemical potential gradients will be practically eliminated at least in the liquid phase.

CIPS Structure Formation When Heat Transport Contributions Prevail. From a simplified point of view, the TIPS and CIPS under same conditions (dope composition and reference temperatures) differ because of the enhanced range of solvent mass transport possibilities in the case of CIPS; for example, transport of solvent can occur in two directions in the case of CIPS (net flow entering the dope (bath → dope) in some instances and leaving the dope (dope → bath) in some other instances) and only in one possible direction (net flow leaving the dope, especially in case of early gelation; see CIPS and processes affecting dope thickness Section) in the case of TIPS. Hence there is possibly a better chance for comparable structural outcomes of CIPS and TIPS when the CIPS membrane structure is largely the outcome of heat transport processes and at that stage mass transport has progressed only to a limited extent.

A situation of the presently considered type might be encountered in the case of the 20 wt % EVOH in 1,3-propanediol and a quench from 80°C to 23 ± 2°C. Any solvent intrusion from the cold bath (in CIPS) is too slow to affect substantially structure formation which is then similar for CIPS and TIPS, and we can approximate the procedure as affected mainly by heat transport; more precisely there is also a mass transport effect but this corresponds to the squeezing of some solvent out of the dope and this, whether limited or not, is common for CIPS and TIPS, and hence, the resulting structures are overall similar ones [Figures 2(b) and 3].

Let us also mention, as partially related and substantially studied already, the bath → dope mass transfer occurring during the precipitation of a dope in a *soft* bath for an ordinary WPI process.[6,8,36] A typical soft bath is one containing a significant fraction of solvent (e.g., 40% FA aqueous solution for the water/FA/Nylon-66 system). In this case, as shown in previous

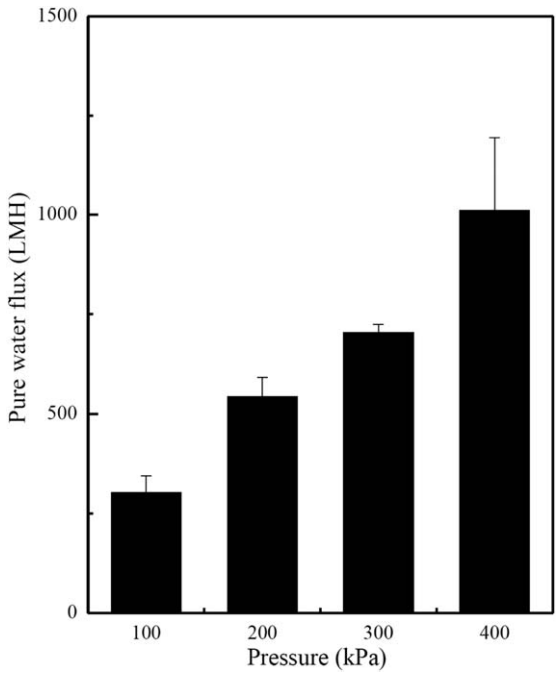

Figure 6. Water fluxes of the EVOH membrane prepared by the CIPS process.

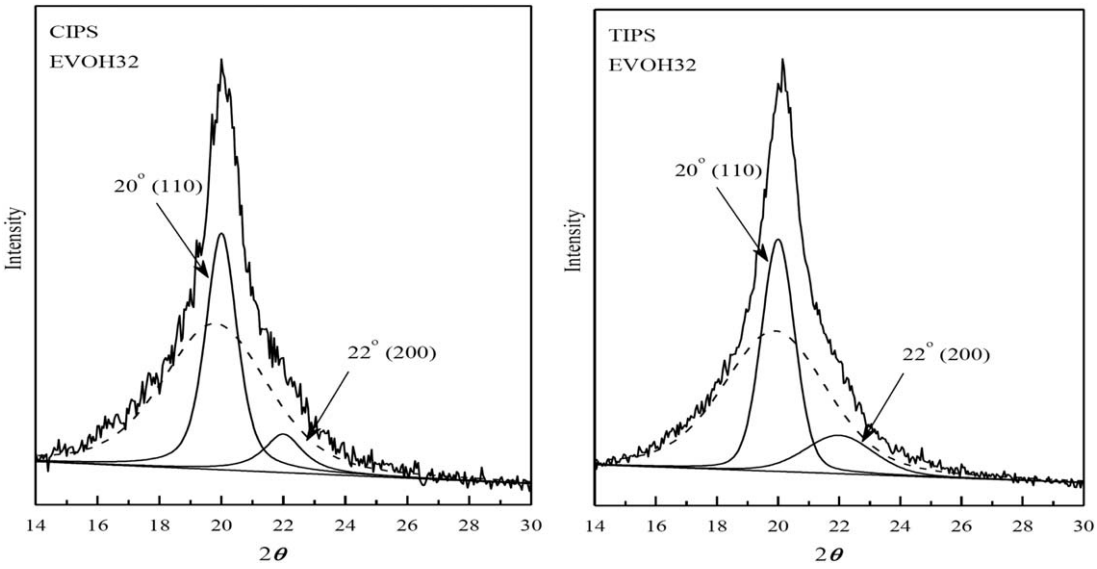

Figure 7. X-ray diffractometer patterns of the EVOH membrane prepared by CIPS and TIPS methods. Amorphous and crystalline regions are sorted by a curve fitting technique.

investigations, the polymer concentration in the dope changed very slowly (typically, it took several tens of seconds for the diffusion trajectory to cross the binodal) and the membrane maintained a relatively flat concentration profile across the cross section during the WPI process.

CIPS Structure Formation Resulting from Comparable Heat and Mass Transport Contributions. There are two ways of having comparable heat and mass transport contributions in the case of CIPS structure formation. One is if mass transport is not diffusional; alternatively structure formation does not progress enough before mass transport, whether diffusional or not, progresses enough. In the case of the FA/Nylon-12 system, the applied quench brings the system below a liquidus but above a buried binodal. Hence the completion of structure formation processes is a slow procedure (because of a large induction period for crystallization and/or slow progress of it after initiation); during this period mass transport between bath and dope, i.e. a procedure not possible for TIPS, continues to modify the composition of the membrane solution. Differences in the mass transport processes for TIPS and CIPS, thus, lead to different dope compositions during structure formation, and this explains the different scales of the two structures in Figure 4. Also during subsequent structure definition, which completes with drying, there is, overall, removal of solvent from the volume defined by the dope (and subsequently by the nascent membrane).

Finally, regardless of the precise transport mechanisms (e.g. diffusion, pressure gradient driven, convection and combinations), the reduced viscosity of the bath liquid (FA compared with 1,3-propanediol) will be a factor in favor of faster mass transport; for example $D \propto \eta^{-0.5}$ to $\eta^{-1.0}$.[37] We now note that FA exhibits a viscosity which is lower by a factor of ca. 30 than that of 1,3-propanediol (ca. 1.6 cp vs. 52 cp) and hence more comparable heat transport and mass transport effects might be expected in the case of the Nylon-12/FA system compared to the EVOH/1,3-propanediol system. As regards heat transfer, it appears that lower viscosity will make simultaneously convective mixing and heat transfer more effective ones. Therefore, for the Formic acid/Nylon-12 system, dope solutions tend to enter the phase separation region more rapidly, in addition to a stronger shift of composition before phase separation occurs.

Properties of the EVOH Membranes

The general properties of the Nylon-12 membrane have been reported.[24] We will now present some information regarding the EVOH membranes prepared via CIPS. In Table II, the porosity, water flux, and tensile strength of the EVOH membrane are summarized to demonstrate the potential applicability of the membrane in fine separation processes. The porosity was ~55% and the nominal pore size as determined from the bubble point method was 1.7 μm, these values suggested that the membrane was suited to micro- and/or ultra-filtration purposes. Water fluxes of the membrane were measured over the transmembrane pressure range of 100–400 kPa, and the results are plotted in Figure 6. Each datum depicts the average value of at least three experimental runs. As is anticipated, the fluxes increase essentially linearly with increasing applied pressure, and they fall over the range of ~300–1000 liter per square meter per hour (LMH). These values are comparable to those of asymmetric poly(vinylidene fluoride) (PVDF) membranes with a nano-porous top surface. The tensile strength at break of the membrane reached 4 N/mm^2; the latter suffices for ordinary micro- and ultra-filtration operations.[8]

The X-ray diffraction pattern of the EVOH membrane is shown in Figure 7. The diffraction peaks at 20.0° and 22.0° correspond to the reflection of (110) and (200) planes of EVOH crystals,[38–40] which verifies crystallization being occurred after L–L demixing during the precipitation process. The diffraction pattern has been decomposed into a broad amorphous halo and sharp peaks by a curve fitting technique, from which the crystallinity was calculated to be 38.8%, a value close to that of EVOH film or fiber reported in the literature.[41, 42]

CONCLUSION

EVOH membranes were prepared by both the conventional TIPS method and the currently developed CIPS method; a comparable lacy-like bi-continuous morphology is obtained from the two methods and, hence, here CIPS offers largely an attractive processing simplification for the fabrication of membranes appropriate for ordinary micro- and ultra-filtration operations. On the other hand, for the Nylon-12/FA system, these two methods generate, for the same conditions, particulate membranes based on particles having volumes differing by one to two orders of magnitude; here CIPS amounts to a method that produces, for the same conditions, a new structure.

Various processes that affect the thickness modification of the dope are described qualitatively for CIPS and TIPS and the differences are pointed out. In addition we describe structure formation by taking into account heat transport and mass transport consequences and distinguish two general cases; the probed EVOH and Nylon-12 systems are representative of the two general possibilities.

ACKNOWLEDGMENTS

The authors thank the Ministry of Science and Technology of Taiwan for the financial support (NSC 99–2221-E-032-002-MY3).

REFERENCES

1. Mulder, M. Basic Principles of Membrane Technology, 2nd Ed.; Kluwer Academic: Dordrecht/Boston/London, **1996**.
2. Beltsios, K.; Steriotis, Th.; Stephanopoulos, K.; Kanellopoulos, N. In Schüth, F., Sing, K., Weitkamp, J., Eds. Handbook of Porous Solids, Vol. *4*, 2281–2433, Wiley-VCH: Weinheim, **2002**.
3. Wang, P. P.; Ma, J.; Wang, Z. H.; Shi, F. M.; Liu, Q. L. *Langmuir* **2012**, *28*, 4776.
4. Zhao, Y. H.; Zhu, B. K.; Kong, L.; Xu, Y. Y. *Langmuir* **2007**, *23*, 5779.
5. Bottino, A.; Cameraroda, G.; Capannelli, G.; Munari, S. *J. Membr. Sci.* **1991**, *57*, 1.
6. Chang, H. H.; Chen, S. C.; Lin, D. J.; Cheng, L. P. *Desalination* **2013**, *313*, 77.
7. Lin, D. J.; Beltsios, K.; Young, T. H.; Jeng, Y. S.; Cheng, L. P. *J. Membr. Sci.* **2006**, *274*, 64.
8. Lin, D. J.; Chang, H. H.; Chen, T. C.; Lee, Y. C.; Cheng, L. P. *Eur. Polym. J.* **2006**, *42* 1581.
9. Lin, D. J.; Chang, C. L.; Huang, F. M.; Cheng, L. P. *Polymer* **2003**, *44*, 413.
10. Ying, L.; Kang, E. T.; Neoh, K. G. *Langmuir* **2002**, *18*, 6416.
11. Hashim, N. A.; Liu, Y. T.; Li, K. *Indus. Eng. Chem. Res.* **2011**, *50*, 3035.
12. Lloyd, D. R.; Kinzer, K. E.; Tseng, H. S. *J. Membr. Sci.* **1990**, *52*, 239.
13. Lim, G. B. A.; Kim, S. S.; Ye, Q. H.; Wang, Y. F.; Lloyd, D. R. *J. Membr. Sci.* **1991**, *64*, 31.
14. Kim, S. S.; Lim, G. B. A.; Alwattari, A. A.; Wang, Y. F.; Lloyd, D. R. *J. Membr. Sci.* **1991**, *64*, 41.
15. Matsuyama, H.; Iwatani, T.; Kitamura, Y.; Tearamoto, M.; Sugoh, N. *J. Appl. Polym. Sci.* **2001**, *79*, 2449.
16. Vadalia, H. C.; Lee, H. K.; Myerson, A. S.; Levon, K. *J. Membr. Sci.* **1994**, *89*, 37.
17. Lloyd, D. R.; Kim, S. S.; Kinzer, K. E. *J. Membr. Sci.* **1991**, *64*, 1.
18. Kim, S. S.; Lloyd, D. R. *J. Membr. Sci.* **1991**, *64*, 13.
19. Matsuyama, H.; Maki, T.; Teramoto, M.; Asano, K. *J. Membr. Sci.* **2002**, *204*, 323.
20. McGuire, K. A.; Laxminarayan, A.; Llyod, D. R. *Polymer* **1994**, *35*, 4404.
21. Caneba, G. T.; Soong, D. S. *Macromolecules* **1985**, *18*, 2538.
22. Safinia, L.; Mantalaris, A.; Bismarck, A. *Langmuir* **2006**, *22*, 3235.
23. Chang, H. H.; Beltsios, K.; Chen, Y. H.; Lin, D. J.; Cheng, L. P. *J. Appl. Polym. Sci.* **2014**, *131*, 40374.
24. Chang, H. H.; Beltsios, K.; Lin, D. J.; Cheng, L. P. *J. Appl. Polym. Sci.* **2013**, *130*, 14.
25. Park, Y. S.; Hatae, T.; Itoh, H.; Jang, M. Y.; Yamazaki, Y. *Electrochim. Acta* **2004**, *50*, 595.
26. Chang, H. H.; Yao, L. C.; Lin, D. J.; Cheng, L. P. *Sep. Puri. Techn.* **2010**, *72*, 156.
27. Daoud, M.; Jannink, G. J. de *Phys.* **1976**, *37*, 973.
28. Kosma, V. A.; Beltsios, K. G. *J. Membr. Sci.* **2012**, *477*, 93.
29. Pinnau, I.; Koros, W. J. *J. Polym. Sci. Polym. Phys.* **1993**, *31*, 419.
30. Semenov, S.; Schimpf, M. *Phys. Rev. E* **2004**, *69*, 011201.
31. Shewmon, P. Diffusion in Solids, Chapter 7, 2nd ed.; Wiley: New York, **1989**.
32. Bird, R. B.; Stewart, W. E.; Lightfoot, E. N. Transport Phenomena, Chapter 9; Wiley: New York, **1960**.
33. Beltsios, K.; Athanasiou, E.; Aidinis, C.; Kanellopoulos, N. *J. Macromol. Sci. Phys. Ed.* **1999**, *38*, 1.
34. Shang, M. X.; Matsuyama, H.; Maki, T.; Teramoto, M.; Lloyd, D. R. *J. Polym. Sci. Polym. Phys.* **2003**, *41*, 194.
35. Caneba, G. T.; Soong, D. S. *Macromolecules* **1985**, *18*, 2545.
36. Cheng, L. P. *Macromolecules* **1999**, *32*, 6668.
37. Reid, R. C.; Prausnitz, J. M.; Sherwood, T. K. The Properties of Gases and Liquids 3rd ed.; McGraw-Hill: New York, **1997**; p. 573.
38. Lopez-Rubio, A.; Lagaron, J. M.; Gimenez, E.; Cava, D.; Hernandez-Munoz, P.; Yamamoto, T.; Gavara, R. *Macromolecules* **2003**, *36*, 9467.
39. Huang, C. H.; Wu, H. M.; Chen, C. C.; Wang, C. W.; Kuo, P. L. *J. Membr. Sci.* **2010**, *353*, 1.
40. Cerrada, M. L.; Perez, E.; Perena, J. M.; Benavente, R. *Macromolecules* **1998**, *31*, 2559.
41. de Lima, J. A.; Felisberti, M. I. *Eur. Polym. J.* **2008**, *44*, 1140.
42. Russo, P.; Acierno, D.; di Maio, L.; Demma, G. *Eur. Polym. J.* **1999**, *35*, 1261.
43. Lagarón, J. M.; Giménez, E.; Saura, J. J.; Gavara, R. *Polymer* **2001**, *42*, 7381.
44. Faisant, J. B.; Aït-Kadi, A.; Bousmina, M.; Deschênes, L. *Polymer* **1998**, *39*, 533.